A Performance Model for an Asynchronous Optical Buffer [1]

W. Rogiest [a,2] K. Laevens [a] D. Fiems [a] H. Bruneel [a]

[a] *SMACS Research Group, Ghent University, Sint-Pietersnieuwstraat 41, B-9000 Ghent, Belgium*

Abstract

We investigate the behaviour of an asynchronous optical buffer by means of a continuous-time queueing model. Through a limit procedure, previously obtained results for a discrete-time queueing model are translated to a continuous-time setting. We also show that the same results can be obtained by a direct analysis using Laplace transforms. Closed-form expressions are obtained for the cases of exponentially distributed burst sizes, deterministic burst sizes and mixtures of deterministic burst sizes.

The performance of asynchronous optical buffers shows the same characteristics as that of synchronous optical buffers: a reduction in throughput due to the creation of voids on the outgoing channel and a burst loss probability that is strongly influenced by the choice of fiber delay line granularity. The optimal value of the latter depends on the burst size distribution and the offered load.

Key words: Burst Switching; Fiber Delay Lines; Loss Probability; Optical Buffers; Generating Functions; Performance Models

1 Introduction

All-optical packet-switching is a promising network technology. Nowadays, major cities are connected by dense wavelength division multiplexing (DWDM)

[1] This document is a post-print of W. Rogiest, K. Laevens, D. Fiems and H. Bruneel, A Performance Model for an Asynchronous Optical Buffer, Performance Evaluation 62 (2005), pp. 313-330.

[2] Supported by the Flemish Government through the IWT-GBOU Project "Optical Networking and Node Architectures".

links, enabling transmission capacities well beyond the Tbit/s. Packet switching over these optical links, however, requires that the transmission speeds over the links are matched by equivalent switching capacities in the nodes. As current packet switches perform data processing in the electronic domain, there is a growing discrepancy between channel capacity and switching capacity. All-optical packet switching (OPS) could alleviate the problem, by processing data in the optical domain [1]. As mature technology is expected to be still a few years away [2], optical burst switching (OBS) has been proposed as an intermediate solution [3, 4, 5].

Both optical packet and optical burst switching suffer from (output port) contention in the switches and therefore equally require contention resolution. Whenever two or more data packets arrive at a network node at the same time and contend for the same output, external blocking occurs. All packets but one are perceived as superfluous, and have to be dealt with. Next to the obvious choice of dropping all excess packets, literature [6, 7] typically presents three solutions: buffering, deflection routing or wavelength conversion. Optical buffering uses fiber delay lines (FDLs) to delay the light, and is regarded as the most effective [7], but comes with the additional cost of the FDLs.

Analytic results concerning the loss and queueing behaviour of optical buffer systems are given in, amongst others, [8, 9, 10]. In [8], an asynchronous FDL buffer with Poisson arrivals of exponentially distributed burst lengths is investigated. Synchronous FDL buffers are studied in [9] and [10] by means of a probability generating functions (pgf's) approach. In particular, the latter paper concerns the performance analysis of a synchronous optical buffer. The results obtained therein will constitute a starting point for our current contribution, dealing with the asynchronous case. Compared to a slotted (i.e., synchronous) network, an unslotted network is expected to be technologically more complex due to control issues. However, an unslotted network could turn out opportune, for reasons of robustness and flexibility. We refer to e.g. [11] for more details. As for the numerical results included in this paper, we remark that, in evaluating the performance of an asynchronous optical buffering, a comparison can be made with the performance of the synchronous case. This comparison is not included here, and we refer to [12] for this approach.

This paper is structured as follows. In the next section, the mathematical model is described and the assumptions we make are given. In Section 3, we derive results for an infinite buffer in equilibrium. We present two approaches, yielding the same results. Either one can use a limit procedure, starting from results for a synchronous system (which are briefly recapitulated), or one can analyze the evolution equation of the asynchronous system directly. In Section 4, heuristics are discussed that allow calculating the burst loss probability in a finite optical buffer, relying on results for the corresponding infinite system. Three special examples of burst size distributions are treated in Section 5.

For these special cases, closed-form expressions for the performance measures of interest are obtained, allowing us to compare the accuracy of the proposed heuristics with simulation results. Conclusions are drawn in Section 6.

2 Model

We study a single outgoing channel, where contention is resolved by means of an FDL buffer. The FDL buffer cannot delay bursts for an arbitrary period of time, but only for multiples of a basic unit D, called the granularity. Buffers of this type are said to be degenerate, and contain $(N+1)$ FDLs with lengths kD for $k = 0, \ldots, N$. Each incoming burst is routed to the shortest of these FDLs such that the burst will not overlap on departure with bursts from the other FDLs. If such an FDL cannot be found, the burst is dropped. In our model, we assume each FDL is a single piece of fiber, which implies that each burst travels through its assigned FDL only once, and that several bursts might be travelling through a single FDL at the same time (without overlapping, however). Further, this puts no limitations on the sizes of the bursts that can be accepted. Other implementations, where e.g. a burst travels in a fixed-length loop of size D for a number of times (as imposed by the scheduling), require less fiber, but can e.g. not delay bursts that are longer than D. This limitation could result in suboptimal performance in some cases, given that the optimal granularity D can be less than the (average) burst size, see below. Also, the number of bursts that can be accepted simultaneously in such structure, is typically upper-bounded by the number of loops that are available.

Typically, bursts are delayed for more time than strictly needed. This extra delay results in so-called voids, i.e., periods during which the output channel remains unused, despite of the fact that the system is not empty. Void-filling policies (VFP) could be used to minimize this loss in throughput, but we do not consider these here.

For ease of analysis, we will assume in Section 3 that the buffer has an infinite amount of FDLs at its disposal, i.e., $N = \infty$. Heuristics are then obtained in Section 4 for finite N, based on the results for $N = \infty$. Studying the system with infinite buffer size, and the evolution over time of its buffer contents, one can distinguish three important variables. Numbering bursts in the order of their arrival, the first variable, the burst inter-arrival time τ_{k}, captures the time between the k^{th} arrival instant and the next. The second variable is the burst size B_{k}, measuring the time needed for transmission of the k^{th} burst. The third important variable is the scheduling horizon H_{k} as observed by the k^{th} burst upon arrival. This quantity represents the time between the instant of arrival, and the earliest instant by which the previous burst (and all its predecessors) will have left the system.

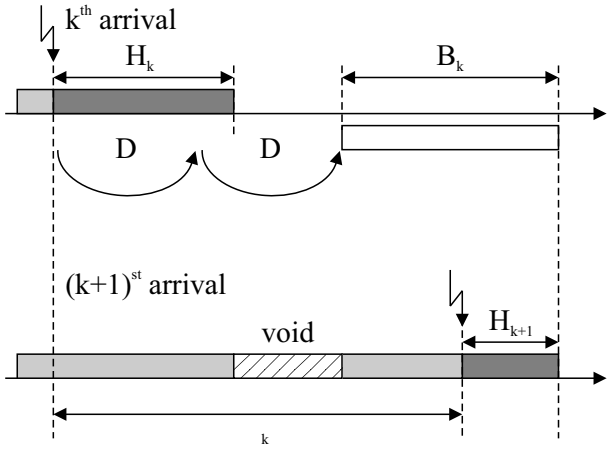

Fig. 1. Evolution of the scheduling horizon H.

The relation between these variables is illustrated in Figure 1, and can be described by the following equation:

$$H_{\mathrm{k}+1} = \left[B_{\mathrm{k}} + D \left\lceil \frac{H_{\mathrm{k}}}{D} \right\rceil - \tau_{\mathrm{k}} \right]^{+} \tag{1}$$

The expression $\lceil x \rceil$ is the ceiling of x, i.e., the smallest integer greater than or equal to x. The notation $[x]^+$ is standard shorthand for $\max(x, 0)$. When the k^{th} burst sees a scheduling horizon H_{k} upon arrival, it will have to be delayed for at least that amount to avoid contention. Since the buffer is degenerate, this delay cannot be realized exactly (in general), the closest match being given by $D \lceil H_{\mathrm{k}}/D \rceil$. Delaying and transmitting this burst pushes the scheduling horizon (just after arrival) to $B_{\mathrm{k}} + D \lceil H_{\mathrm{k}}/D \rceil$. Taking then into account the burst inter-arrival time τ_{k}, and the possibility that the system becomes empty, one easily obtains equation (1). Note that it is valid for both continuous-time (CT) and discrete-time (DT) systems.

To analyze equation (1), we need to impose certain restrictions on the distribution of τ_{k} and B_{k}. We assume the τ_{k} to form a sequence of iid (independent and identically distributed) random variables (rv's), having a common memoryless distribution. The burst sizes B_{k} also form a sequence of iid rv's, and can have a general distribution. In the below, every time both CT and DT variables occur under the same name, we denote DT variables with a prime, e.g. D', and leave CT variables unchanged, e.g. D. In DT, we will use the probability generating function (pgf) of the probability mass function (pmf), in CT we use the Laplace-Stieltjes transform (LST) of the probability density function (pdf). For the burst sizes B_{k}, this means we have

$$B(z) = \mathrm{E}[z^{B'_{\mathrm{k}}}] = \sum_{\mathrm{n}=1}^{\infty} z^n \Pr[B'_{\mathrm{k}} = n]$$

and

$$B^*(s) = \mathrm{E}[\mathrm{e}^{-sB_\mathrm{k}}] = \int_0^\infty \mathrm{e}^{-sx}\, b(x)dx$$

As for the inter-arrival times, being memoryless, we have a geometric distribution in DT, with mean $1/p$, and an exponential distribution in CT, with arrival intensity λ,

$$\Pr[\tau'_\mathrm{k} = n] = p \cdot \bar{p}^{n-1}\,,\ n = 1, 2, ... \quad \text{and} \quad \Pr[\tau_\mathrm{k} \le x] = 1 - \mathrm{e}^{-\lambda x}\,,\ x \ge 0$$

(We use the standard notation $\bar{p} = 1 - p$.) The expressions for the corresponding pgf and Laplace transform are

$$\tau(z) = \mathrm{E}[z^{\tau'_\mathrm{k}}] = \frac{pz}{1 - \bar{p}z} \quad \text{and} \quad \tau^*(s) = \mathrm{E}[\mathrm{e}^{-s\tau_\mathrm{k}}] = \frac{\lambda}{\lambda + s}$$

3 Analysis

In this section, we take a look at the infinite system. All derivations assume the system is stable. On this condition, the distributions of H_k converge, for $k \to \infty$, to a unique stochastic equilibrium distribution, independent of the initial system conditions. The pgf and Laplace transforms obtained are associated with this equilibrium. By H we will denote a generic rv following that distribution (and likewise for other rv's involved). Stability requires the offered load ρ to be below some maximum value ρ_max, that is, typically less than unity, unlike in conventional queues, see e.g. [13]. This is also commented upon below.

We present two approaches to obtain, among others, the Laplace transform of H in the continuous-time setting. One consists in taking appropriate limits for the slot size becoming infinitely small, mapping results from the discrete-time setting to the continuous-time setting. The other consists in directly analyzing the evolution equation (1) in continuous time. Before continuing, we note that two separate non-linear effects can be observed in (1): the operation $[x]^+$ and $\lceil x \rceil$. The former effect, related to the non-negativeness of the buffer content, one could call the queueing effect, and requires us to analyze $H = [B + F - \tau]^+$. The latter effect, related to the finite granularity of the FDLs, one could call the FDL effect, and calls for analysis of $F = D \left\lceil \frac{H}{D} \right\rceil$. Note how values of H are mapped to multiples of D. Below, we will refer to the former effect as "the queueing effect" and to the latter as "the FDL effect" respectively. Both will first be analyzed separately. Results will then be combined to yield the overall solution.

3.1 Results for synchronous systems

In [10], both the queueing effect $[x]^+$ and the FDL effect $\lceil x \rceil$ were studied in a discrete-time setting. The queueing effect yielded the following relation between the pgfs of the variables involved:

$$H(z) = \frac{p}{z-\bar{p}} B(z) F(z) + K' \frac{z-1}{z-\bar{p}} \tag{2}$$

The FDL effect leads to following relation:

$$F(z) = \sum_{\mathrm{k}} \frac{1}{D'} \frac{z^{D'}-1}{z\epsilon_{\mathrm{k}}-1} H(z\epsilon_{\mathrm{k}}) \tag{3}$$

where symbols $\epsilon_{\mathrm{k}} = \mathrm{e}^{\mathrm{j}\,2\pi k/D'}$ represent the D' different complex D'$^{\text{th}}$ roots of unity, and the summation index k runs over $-D'/2 < k \leq D'/2$ (taking on integer values only). Note that in [10], the summation ran over $0 \leq k < D'$. For our present purposes, however, using $-D'/2 < k \leq D'/2$, turns out to be more convenient.

Using the property that $F(z\epsilon_{\mathrm{k}}) = F(z)$, which follows directly from the fact that the random variable F is always an integer multiple of D', one can combine (2) and (3). With the identity

$$\frac{x^{D'-1}}{z^{D'}-x^{D'}} = \sum_{\mathrm{k}} \frac{1}{D'} \frac{1}{(z\epsilon_{\mathrm{k}})-x} \tag{4}$$

the expression simplifies to

$$F(z) = K' \left(\frac{\bar{p}^{D'-1}(z^{D'}-1)}{z^{D'}-\bar{p}^{D'}} \right) \cdot \left(1 - \sum_{\mathrm{k}} \frac{1}{D'} \cdot \frac{z^{D'}-1}{z\epsilon_{\mathrm{k}}-1} \frac{pB(z\epsilon_{\mathrm{k}})}{(z\epsilon_{\mathrm{k}})-\bar{p}} \right)^{-1} \tag{5}$$

The constant K' follows from the normalization condition $F(1) = 1$, as

$$K' = \left(\frac{1}{p} - \mathrm{E}[B'] - \frac{D'-1}{2} - \sum_{\mathrm{k}\neq 0} \frac{1}{\epsilon_{\mathrm{k}}-1} \frac{p}{\epsilon_{\mathrm{k}}-\bar{p}} B(z\epsilon_{\mathrm{k}}) \right) \cdot \left(\frac{D\bar{p}^{D'-1}}{1-\bar{p}^{D'}} \right)^{-1}$$

Having determined $F(z)$, $H(z)$ then follows readily from (2).

3.2 Limit procedure

Our scope is to derive, for the asynchronous system, $H^*(s)$, the LST of the equilibrium distribution of the scheduling horizon H as seen by arrivals. In this subsection, we discuss a limit procedure, to retrieve $H^*(s)$ from $H(z)$.

To correctly convert results from discrete time to continuous time, one should first observe quantities in the discrete domain. A distinction can be made between time-related quantities and counting-related quantities. The former scale with the slot size Δ, the latter do not. For example, the scheduling horizon H' (in slots) actually represents $H'\Delta$ in absolute time. We can also find a simple relation between the pgf and LST, as

$$H^*(s) = \mathrm{E}[\mathrm{e}^{-sH}] = \lim_{\Delta \to 0} \mathrm{E}[(\mathrm{e}^{-s\Delta})^{H'}] = \lim_{\Delta \to 0} H(\mathrm{e}^{-s\Delta})$$

i.e., we need to substitute z by $\mathrm{e}^{-s\Delta}$ in the pgf $H(z)$ before taking the limit $\Delta \to 0$. The average inter-arrival time $1/p$ scales as $1/(\lambda\Delta)$, the granularity size as $D'\Delta = D$. Applying this limit procedure on the DT solution (2) for the queueing effect yields

$$H^*(s) = \frac{\lambda}{\lambda - s} F^*(s) B^*(s) - K \frac{s}{\lambda - s} \tag{6}$$

(In taking the limit, here and in the following, the rules of de l'Hôpital need to be applied frequently, to deal with e.g. indeterminate forms of type 0/0.)

Concerning the FDL effect, equation (3) results in

$$F^*(s) = \sum_{\mathrm{k}} \frac{1}{D} \frac{1 - \mathrm{e}^{-sD}}{s + \mathrm{j}\, 2\pi k/D} H^*(s + \mathrm{j}\, 2\pi k/D) \tag{7}$$

where k now runs from $-\infty$ to $+\infty$.

Note that $F^*(s)$ is periodical too, in the sense that

$$F^*(s) = F^*(s + \mathrm{j}\, 2\pi n/D)$$

for any $n \in \mathbb{Z}$. This property now allows combining (6) and (7) to yield

$$\begin{aligned} F^*(s) = & \left(-K \sum_{\mathrm{k}} \frac{1}{D} \frac{1 - \mathrm{e}^{-sD}}{\lambda - (s + \mathrm{j}\, 2\pi k/D)} \right) \\ & \cdot \left(1 - \sum_{\mathrm{k}} \frac{1}{D} \frac{1 - \mathrm{e}^{-sD}}{t} \frac{\lambda B^*(t)}{\lambda - t} \bigg|_{t = s + \mathrm{j}\, 2\pi k/D} \right)^{-1} \end{aligned} \tag{8}$$

A further simplification can be made by using

$$\sum_{\mathrm{k}} \frac{1}{D} \frac{1}{\lambda - (s + \mathrm{j}\, 2\pi k/D)} = -\frac{1}{1 - \mathrm{e}^{(\lambda - s)d}} \tag{9}$$

which follows from applying the limit procedure on (4) (where $x = 1$). We

then find

$$F^*(s) = \left(K \frac{1 - \mathrm{e}^{-sD}}{1 - \mathrm{e}^{(\lambda - s)D}} \right) \cdot \left(1 - \sum_{\mathrm{k}} \frac{1}{D} \frac{1 - \mathrm{e}^{-sD}}{t} \frac{\lambda B^*(t)}{\lambda - t} \Big|_{t = s + \mathrm{j}\, 2\pi k/D} \right)^{-1} \quad (10)$$

This is exactly the expression we would have found applying the limit procedure directly to equation (5).

The remaining unknown constant K can be determined, either by applying the limit procedure once more, or by ensuring normalization of $F^*(s)$. The final result reads

$$K = \left(\frac{1}{\lambda} - \mathrm{E}[B] - \frac{D}{2} - \sum_{\mathrm{k} \neq 0} \frac{\lambda}{t - \lambda} \frac{B^*(t)}{t} \Big|_{t = s + \mathrm{j}\, 2\pi k/D} \right) \cdot \left(- \frac{D}{1 - \mathrm{e}^{-\lambda D}} \right)^{-1} \quad (11)$$

Equations (6), (10) and (11) together fully specify $H^*(s)$.

3.3 Direct approach

To consolidate the results of Subsection 3.2, we show how they can also be obtained directly. The complexity of the transform-based solution of the queueing effect, mentioned in the above, critically depends on the exact form of the LST of τ. (The same goes, in terms of the pgf of τ, for the discrete-time case, as discussed in e.g. [14].) For exponentially distributed τ, the complexity is limited, and results in

$$H^*(s) = \frac{\lambda}{\lambda - s} B^*(s) F^*(s) - K \frac{s}{\lambda - s}$$

i.e., the result we obtained via the limit procedure. A direct proof is rather straightforward. Introducing, for convenience, an auxiliary rv $G = B + F$, with pdf $g(t)$ $(t > 0)$ and LST $G^*(s) = B^*(s) F^*(s)$, one has

$$
\begin{aligned}
H^*(s) &= \int_0^\infty g(t)dt \int_0^\infty \tau(x)dx \ \mathrm{e}^{-s[t-x]^+} \\
&= \int_0^\infty g(t)dt \int_0^\infty \tau(x)dx \ \mathrm{e}^{-s(t-x)} \\
&\quad + \int_0^\infty g(t)dt \int_t^\infty \tau(x)dx \left(\mathrm{e}^{-s\cdot 0} - \mathrm{e}^{-s(t-x)}\right) \\
&= G^*(s)\tau^*(-s) + \int_0^\infty g(t)dt \int_t^\infty \lambda \, \mathrm{e}^{-\lambda x} \, dx \left(1 - \mathrm{e}^{-st} \, \mathrm{e}^{+sx}\right) \\
&= G^*(s)\frac{\lambda}{\lambda - s} + \int_0^\infty g(t)dt \left(\mathrm{e}^{-\lambda t} - \mathrm{e}^{-st} \, \frac{\lambda}{\lambda - s} \, \mathrm{e}^{-(\lambda - s)t}\right) \\
&= G^*(s)\frac{\lambda}{\lambda - s} + G^*(\lambda)\left(1 - \frac{\lambda}{\lambda - s}\right) \\
&= G^*(s)\frac{\lambda}{\lambda - s} - K\frac{s}{\lambda - s}
\end{aligned}
$$

The second non-linearity to tackle, is the FDL effect, as stated above. The transform-based solution can be obtained by expressing $F^*(s)$ as

$$
F^*(s) = h(0) + \sum_{\mathrm{k}=0}^{+\infty} \int_{0^+}^{D} h(u + kD) \, \mathrm{e}^{-s(k+1)D} \, du
$$

Rewriting the sum in the right-hand side by introducing the comb function $\sum_{\mathrm{l}} \delta\langle t - lD\rangle$ we have

$$
\begin{aligned}
F^*(s) &= h(0) + \sum_{\mathrm{k}=0}^{+\infty} \int_{0^+}^{D} du \, h(u + kD) \, \mathrm{e}^{-s(k+1)D} \\
&\quad \cdot \int_{0^+}^{D} dx \ \mathrm{e}^{-s(u-x)} \sum_{\mathrm{l}=-\infty}^{+\infty} \delta\langle (u - x) - lD\rangle
\end{aligned}
$$

Note that the only Dirac pulse actually having an effect is the one for $u-x = 0$, i.e., for $l = 0$. Using the Fourier expansion

$$
\sum_{\mathrm{k}=-\infty}^{+\infty} \delta\langle x - kD\rangle = \sum_{\mathrm{k}=-\infty}^{+\infty} \frac{1}{D} \ \mathrm{e}^{\mathrm{j}\, 2\pi kx/D}
$$

and rearranging some terms, we can proceed as

$$
\begin{aligned}
F^*(s) &= h(0) + \sum_{\mathrm{k}=0}^{+\infty} \int_{0^+}^{D} du\, h(u+kD)\, \mathrm{e}^{-s(k+1)D} \\
&\quad \cdot \int_{0^+}^{D} dx\ \mathrm{e}^{-s(u-x)} \sum_{\mathrm{l}=-\infty}^{+\infty} \frac{1}{D}\ \mathrm{e}^{-\mathrm{j}\,2\pi l(u-x)/D} \\
&= h(0) + \mathrm{e}^{-sD} \int_{0^+}^{D} dx \sum_{\mathrm{l}=-\infty}^{+\infty} \frac{1}{D}\ \mathrm{e}^{(s+\mathrm{j}\,2\pi l/D)x} \\
&\quad \cdot \sum_{\mathrm{k}=0}^{+\infty} \int_{0^+}^{D} du\, h(u+kD)\, \mathrm{e}^{-s(u+kD)-\mathrm{j}\,2\pi lu/D} \\
&= h(0) + \mathrm{e}^{-sD} \sum_{\mathrm{l}=-\infty}^{+\infty} \frac{1}{D} \frac{\mathrm{e}^{(s+\mathrm{j}\,2\pi l/D)D} - 1}{s+\mathrm{j}\,2\pi l/D} \\
&\quad \cdot \sum_{\mathrm{k}=0}^{+\infty} \int_{0^+}^{D} du\, h(u+kD)\, \mathrm{e}^{-(s+\mathrm{j}\,2\pi l/D)\cdot(u+kD)}
\end{aligned}
$$

In the last step we used the obvious identity

$$
\mathrm{e}^{-(\mathrm{j}\,2\pi l/D)kD} = 1
$$

for any $l, k \in \mathbb{Z}$, which allowed us to arrive at an expression in terms of $u+kD$ only in the integral for u. That integration then, combined with the sum over k, amounts to integrating over $(0, \infty)$, i.e.,

$$
\begin{aligned}
F^*(s) &= h(0) + \mathrm{e}^{-sD} \sum_{\mathrm{l}=-\infty}^{+\infty} \frac{1}{D} \frac{\mathrm{e}^{(s+\mathrm{j}\,2\pi l/D)D} - 1}{s+\mathrm{j}\,2\pi l/D} \int_{0^+}^{\infty} dt\, h(t)\, \mathrm{e}^{-(s+\mathrm{j}\,2\pi l/D)t} \\
&= h(0) + \sum_{\mathrm{l}=-\infty}^{+\infty} \frac{1}{D} \frac{1-\mathrm{e}^{-sD}}{s+\mathrm{j}\,2\pi l/D} \left(H^*(s+\mathrm{j}\,2\pi l/D) - h(0)\right)
\end{aligned}
$$

Using identity (9) once more, we find that the terms involving $h(0)$ cancel out, yielding

$$
F^*(s) = \sum_{\mathrm{l}} \frac{1}{D} \frac{1-\mathrm{e}^{-sD}}{s+\mathrm{j}\,2\pi l/D} H^*(s+\mathrm{j}\,2\pi l/D)
$$

as before.

4 Heuristics for the burst loss probability

Results up to now related to an optical buffer of infinite size. In order to obtain the burst loss probability (BLP) in a finite system, i.e., a system with only $(N+1)$ fiber delay lines (realizing delays in the set $\{0, D, \ldots, ND\}$) one can rely on heuristics, as explained next.

For conventional queues, fed by a Poisson process of bursts of iid size, a relation exists between (the distributions of) the unfinished work in an infinite system and that in a finite system of, say, capacity M, see e.g. [15]. This relation leads to an expression for the loss ratio (LR) in the finite system of the form

$$LR = \frac{(1-\rho)}{\rho} \frac{\Pr[W_\infty > M]}{1 - \Pr[W_\infty > M]} \tag{12}$$

where W_∞ denotes the unfinished work in the infinite system (as seen by arrivals). When dealing with degenerate buffers, one can translate this into a heuristic for the BLP

$$BLP \approx \frac{(1-\rho_{\rm eq})}{\rho_{\rm eq}} \frac{\Pr[H_\infty > ND]}{1 - \Pr[H_\infty > ND]} \tag{13}$$

Here, H_∞, the scheduling horizon in an infinite optical buffer, fulfills the role of W_∞, ND is the capacity of the system and $\rho_{\rm eq}$ is the so-called equivalent load, i.e., the load on the system taking into account the overhead created by the voids. (Note that formula (12) assumes only excess unfinished work is lost, i.e., bursts arriving at a nearly full system can still be partially buffered, while in our model, a burst that cannot be delayed sufficiently long due to lack of an appropriate delay line, is dropped entirely.)

We can again combine results of the synchronous FDL buffer [10] with the limit procedure to find expressions for the unknown quantities $\rho_{\rm eq}$ and $\Pr[H_\infty > ND]$ in heuristic (13).

The equivalent load in the synchronous setting is given by

$$\rho'_{\rm eq} = p \left(\mathrm{E}[B'] + \frac{D'-1}{2} + \sum_{\mathrm{k}\neq 0} \frac{1}{\epsilon_\mathrm{k} - 1} \frac{pB(\epsilon_\mathrm{k})}{\epsilon_\mathrm{k} - \bar{p}} \right) \tag{14}$$

The limit procedure then easily leads to the equivalent load in the asynchronous setting. One finds

$$\rho_{\rm eq} = \lambda \left(\mathrm{E}[B] + \frac{D}{2} + \sum_{\mathrm{k}\neq 0} \frac{\lambda}{t-\lambda} \left. \frac{B^*(t)}{t} \right|_{t=s+\mathrm{j}\,2\pi k/D} \right)$$

The equivalent load thus involves the mean burst size, (about) half the delay line granularity, and a term taking into account the finer details of the burst size distribution (through its pgf $B(z)$ or LST $B^*(t)$). One can show that the asynchronous system becomes unstable when λ is such that $\rho_{\rm eq} = 100\%$.

The tail probabilities $\Pr[H_\infty > ND]$ that appear in heuristic (13) can be computed by an (approximate) inversion of the LST $H^*(s)$, using a single-pole approximation. It was shown in [10] that for synchronous buffers one

has

$$\Pr[H_\infty > ND'] \approx \frac{cst'}{z_0^{ND'}}$$

Here, z_0 is the dominant pole of $H(z)$ (and of $F(z)$). It is real, positive and larger than 1. This approximate geometric behaviour occurs under rather mild conditions on the burst size distribution, a sufficient condition is e.g. for the burst size pgf to be a rational function. Note, however, that the analysis in e.g. Section 3 only requires that $\mathrm{E}[B] < \infty$ (and that the system is stable). When, for instance, the burst size distribution possesses a heavy tail, the distribution of H_∞ would not decay geometrically as above, but would have a heavy tail too. This would require a different approximate inversion formula.

The constant cst' follows from residue theory and is given by

$$cst' = -\frac{1}{z_0}\frac{D'}{z_0^{D'}-1}\left(\lim_{z\to z_0} F(z)(z-z_0)\right)$$

Applying the limit procedure once more, we find that for asynchronous buffers

$$\Pr[H_\infty > ND] \approx \frac{cst}{\gamma^N}$$

where we introduced $\gamma = \mathrm{e}^{-s_0 D} = \lim_{\Delta\to 0} z_0^{D'}$ for convenience. Here, s_0 denotes the dominant pole of $H^*(s)$ and $F^*(s)$ along the negative real line. In general, a simple bisection algorithm (with possibly an initial search for the appropriate starting interval) suffices to determine γ numerically. In some cases, an explicit expression can also be found, see e.g. below.

For small BLP, a modified heuristic

$$BLP \approx (1-\rho_{\mathrm{eq}})\frac{\Pr[H_\infty > ND]}{1-\Pr[H_\infty > ND]} \tag{15}$$

(i.e., dropping the factor ρ_{eq} in the denominator) turns out to be more accurate. In the following, we will refer to (13) as "heuristic A" and to (15) as "heuristic B" respectively.

It is worth to point out that the same heuristics can also be used to evaluate the BLP in overloaded systems, i.e., when the equivalent load exceeds 100%. Strictly speaking, no equilibrium distribution then exists for e.g. H_∞. The transform $H^*(s)$ that is used to approximate $\Pr[H_\infty > ND]$, however, remains a proper function. Formally then, one can still compute the quantities $\Pr[H_\infty > ND]$, the only caveat being that γ is then to be found in the interval $[0, 1)$, i.e. $s_0 > 0$. The expression for the constant cst remains the same. (When the equivalent load is exactly 100%, $s_0 = 0$ and $\gamma = 1$. In principle, this requires somewhat modified expressions. Here, we do not pursue this issue further.)

For severely overloaded systems, there is a rather simple, intuitive heuristic. In e.g. conventional queues, when $\rho \to \infty$, the loss ratio will approximately equal

$$LR \approx \frac{\rho - 1}{\rho}$$

Since such a system will be busy nearly always, the carried load will be close to one. The lost load then equals $\rho - 1$, leading directly to the above approximation. As $\rho \to \infty$, the (formal) value for $\Pr[W_\infty > M] \to \infty$, thus the same limit is retrieved in formula (12). Not surprisingly then, for degenerate buffers, heuristic A turns out to be more accurate than heuristic B when $\rho_{\text{eq}} \gg 1$. This will be illustrated shortly by means of a few numerical examples.

5 Special cases

In this section, we take a look at the BLP for three special cases for the burst size distribution: exponential, deterministic and a mixture of deterministics. For all three of them, the infinite sum appearing in a.o. equations (10) and (11), can be removed. One obtains closed-form formulas for the LST $H^*(s)$ and for the performance measures derived therefrom. Results given here were obtained via the limit procedure. Formulas for the corresponding discrete-time systems are given in [16]. Their derivation relied on identities resulting from the partial fraction expansion of appropriately constructed rational functions. At the time of writing, we were unable to verify whether similar identities (involving infinite sums) can be used to simplify e.g. equation (5) for $F^*(s)$ directly. Here, we merely state the important formulae, especially focussing on those needed in the above mentioned heuristics for the BLP.

5.1 Exponentially distributed burst sizes

As was the case for the inter-arrival times τ, exponentially distributed burst sizes can be considered as the limit (for slot sizes going to zero) of geometrically distributed burst sizes. If we denote the mean burst size by the standard notation $\mathrm{E}[B] = \mu^{-1}$, the LST of the burst size distribution then takes on the well-known form $B(s) = \frac{\mu}{\mu+s}$. Expression (10) for $F^*(s)$ simplifies significantly to

$$F^*(s) = \frac{1 - \mathrm{e}^{-(s+\mu)D}}{1 - \mathrm{e}^{-\mu D}} \cdot \frac{\gamma - 1}{\gamma - \mathrm{e}^{-sD}} \quad \text{with } \gamma = \frac{\mu + \lambda}{\mu\,\mathrm{e}^{-\mu D} + \lambda\,\mathrm{e}^{+\lambda D}}$$

The constant *cst* appearing in the approximation for the tail distribution becomes

$$cst = \frac{1 - \gamma\,\mathrm{e}^{-\mu D}}{\gamma\,(1 - \mathrm{e}^{-\mu D})}$$

We further obtain

$$\rho_{\text{eq}} = 1 + \frac{\lambda D}{\mu + \lambda} \left(\frac{\lambda}{1 - \mathrm{e}^{-\mu D}} + \frac{\mu}{1 - \mathrm{e}^{+\lambda D}} \right)$$

for the equivalent load.

A similar expression was found in e.g. [17]. In that paper, the authors derive an expression for the LST of the distribution of the equivalent burst size B_{eq}, i.e., the burst size taking into account the voids created due to the degenerate structure of the FDL buffer. The analysis proceeds along somewhat different lines than followed here, but results for e.g. the equivalent load are the same. No explicit expression was derived for the LST of the scheduling horizon, however. Taking the LST of B_{eq} as the authors obtained it, and using it in the classical Pollaczek-Khinchin formula for the unfinished work in the M/G/1 system, see e.g. [18], does not yield $H^*(s)$ as given here. This comes as no surprise, given that the equivalent burst size depends on the scheduling horizon as seen by the arriving burst, i.e., we are not dealing with a conventional M/G/1 system here. Rewriting equation (1) as

$$H_{\text{k+1}} = [H_{\text{k}} + B_{\text{eq,k}} - \tau_{\text{k}}]^+ \quad \text{with} \quad B_{\text{eq,k}} = B_{\text{k}} + D \left\lceil \frac{H_{\text{k}}}{D} \right\rceil - H_{\text{k}}$$

the dependence between H_{k} and $B_{\text{eq,k}}$ explicitly shows up.

Note further that, in this case, it is straightforward to verify that

$$\rho_{\text{eq}} = 1 \Leftrightarrow \gamma = 1 \Leftrightarrow s_0 = 0$$

as mentioned above. The condition under which $\rho_{\text{eq}} = 1$ fully agrees with the one that can be found by taking the appropriate limit of the condition derived in [13] for the synchronous case.

With these formulas at hand, one can easily calculate the BLP via one of the heuristics given above. Some numerical results are shown in Figure 2. It compares results from simulation (points connected by dotted lines) with those obtained via heuristic A (solid gray curves) or heuristic B (solid black curves). The mean burst size $\mathrm{E}[B]$ was set to 50 μs, which corresponds to circa 60 kbytes at 10 Gbps. The granularity D varied from 0 to 100 μs (in steps of 5 μs during the simulations). The number of available FDLs was set to $N = 20$. The figure shows results for different input load levels $\rho = \lambda \mathrm{E}[B]$.

The heuristics are a bit pessimistic, i.e., they overestimate the BLP. Heuristic B is more accurate for low input load levels, but does not converge to the right asymptotic value when $\rho_{\text{eq}} \gg 1$, as predicted. (Here, $\rho_{\text{eq}} \to \infty$ as $D \to \infty$). For these high loads, heuristic A performs better. Compared to the method discussed in [8], one gains somewhat in accuracy, especially for low load values

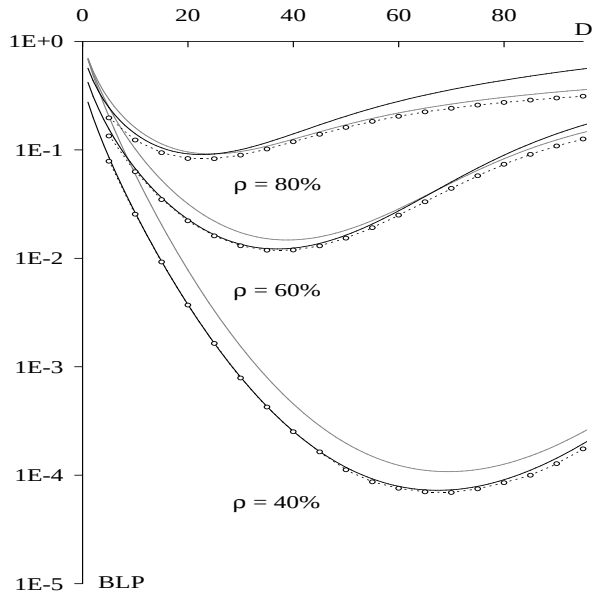

Fig. 2. BLP for exponentially distributed burst sizes ($N = 20$).

or small buffer sizes. Furthermore, since for this special case, explicit formulae were obtained, the numerical complexity involved in our results is close to zero.

There is an optimal granularity D (in terms of BLP) , shifting to lower values for higher input load levels, as was the case in synchronous systems, see [10]. As we will illustrate next, the optimal value also depends on the burst size distribution.

5.2 Deterministic burst sizes

In this case, all burst are of length B. In order to proceed, we need to express B as $aD - b$, where $a \geq 1$ and $0 \leq b < D$. That is, $a = \lceil B/D \rceil$ and $b = aD - B$. With this convention, the limit procedure yields

$$F^*(s) = \frac{-\left(a\left(1-\mathrm{e}^{-\lambda D}\right)-\mathrm{e}^{-\lambda(D-b)}\right)\left(1-\mathrm{e}^{-sD}\right)}{\mathrm{e}^{-saD}\,\mathrm{e}^{-\lambda(D-b)}\left(1-\mathrm{e}^{-sD}\right)+\left(\mathrm{e}^{-\lambda D}-\mathrm{e}^{-sD}\right)\left(1-\mathrm{e}^{-saD}\right)}$$

The equivalent load is now given by

$$\rho_{\mathrm{eq}} = 1 + \lambda D\left(a - \frac{\mathrm{e}^{-\lambda(D-b)}}{1-\mathrm{e}^{-\lambda D}}\right)$$

and reaches 100% when

$$a = \frac{\mathrm{e}^{-\lambda(D-b)}}{1-\mathrm{e}^{-\lambda D}}$$

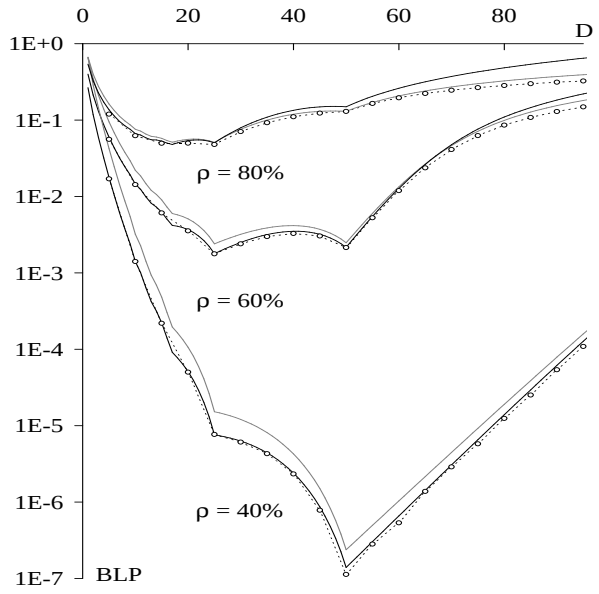

Fig. 3. BLP for deterministic burst sizes ($N = 20$).

again in agreement with what one would obtain by taking the appropriate limit of the condition given in [13] for this specific case.

The dominant pole $\gamma = \mathrm{e}^{-s_0 D}$ now has to be determined as the solution of

$$\gamma^a \, \mathrm{e}^{-\lambda(D-b)}(1-\gamma) + (\mathrm{e}^{-\lambda D} - \gamma)(1-\gamma^a) = 0$$

For $\rho_{\mathrm{eq}} < 100\%$ it is the solution in $(1, \infty)$, for $\rho_{\mathrm{eq}} > 100\%$ it is the solution in $(0, 1)$.

Finally, the constant needed in the approximation of $\Pr[H_\infty > ND]$ is given by

$$cst = \frac{-\left(a\left(1-\mathrm{e}^{-\lambda D}\right) - \mathrm{e}^{-\lambda(D-b)}\right)}{a\gamma^a(\gamma - \mathrm{e}^{-\lambda D}) - \gamma(1-\gamma^a) - \gamma^a(\gamma + \gamma a - a)\,\mathrm{e}^{-\lambda(D-b)}}$$

Some results for this case are given in Figure 3, which shows similar curves as in Figure 2. Again, the (mean) burst size was set to 50 μs, the granularity D varied from 0 to 100 μs, and the number of available FDLs was set to $N = 20$. The shape of the curves is substantially different from the ones in Figure 2, and the BLP can be more than an order of magnitude smaller. Again, heuristic B is more accurate for lower values of the BLP, but does not converge to the correct limit for $\rho_{\mathrm{eq}} \gg 1$. There are now several "local optima", when B is a multiple of D, i.e., for $b = 0$. The global optimum value of D is again function of the load, but not in a continuous fashion, as was the case for exponentially distributed burst sizes.

5.3 Mixtures of deterministic burst sizes

It is rather straightforward to extend the above results to mixtures of e.g. deterministic burst sizes. Burst lengths then take on a limited number of values B_i ($i = 1, \ldots, R$) with probabilities α_i ($\sum \alpha_\mathrm{i} = 1$). We again express each B_i as $a_\mathrm{i} D - b_\mathrm{i}$ as above. The limit procedure results in

$$F^*(s) = -\left(\sum_{\mathrm{i}=1}^{\mathrm{R}} \alpha_\mathrm{i} \left\{\left(a_\mathrm{i}\left(1-\mathrm{e}^{-\lambda D}\right) - \mathrm{e}^{-\lambda(D-b_\mathrm{i})}\right)\left(1-\mathrm{e}^{-sD}\right)\right\}\right)$$
$$\cdot \left(\sum_{\mathrm{i}=1}^{\mathrm{R}} \alpha_\mathrm{i} \left\{\mathrm{e}^{-sa_\mathrm{i}D}\,\mathrm{e}^{-\lambda(D-b_\mathrm{i})}\left(1-\mathrm{e}^{-sD}\right) + \left(\mathrm{e}^{-\lambda D} - \mathrm{e}^{-sD}\right)\left(1-\mathrm{e}^{-sa_\mathrm{i}D}\right)\right\}\right)^{-1}$$

and

$$\rho_{\mathrm{eq}} = 1 + \lambda D \left(\sum_{\mathrm{i}=1}^{\mathrm{R}} \alpha_\mathrm{i} \left\{a_\mathrm{i} - \frac{\mathrm{e}^{-\lambda(D-b_\mathrm{i})}}{1-\mathrm{e}^{-\lambda D}}\right\}\right)$$

The dominant pole $\gamma = \mathrm{e}^{-s_0 D}$ has to be determined from

$$\sum_{\mathrm{i}=1}^{\mathrm{R}} \alpha_\mathrm{i} \left\{\gamma^{a_\mathrm{i}}\,\mathrm{e}^{-\lambda(D-b_\mathrm{i})}(1-\gamma) + (\mathrm{e}^{-\lambda D} - \gamma)(1-\gamma^{a_\mathrm{i}})\right\} = 0$$

The constant needed in the approximation of $\Pr[H_\infty > ND]$ is given by

$$cst = \frac{-\sum_{\mathrm{i}=1}^{\mathrm{R}} \alpha_\mathrm{i} \left\{a_\mathrm{i}\left(1-\mathrm{e}^{-\lambda D}\right) - \mathrm{e}^{-\lambda(D-b_\mathrm{i})}\right\}}{\sum_{\mathrm{i}=1}^{\mathrm{R}} \alpha_\mathrm{i} \left\{a_\mathrm{i}\gamma^{a_\mathrm{i}}(\gamma - \mathrm{e}^{-\lambda D}) - \gamma(1-\gamma^{a_\mathrm{i}}) - \gamma^{a_\mathrm{i}}(\gamma + \gamma a_\mathrm{i} - a_\mathrm{i})\,\mathrm{e}^{-\lambda(D-b_\mathrm{i})}\right\}}$$

Results for $R = 2$ are shown in Figure 4. Burst sizes were $B_1 = 45$ μs and $B_2 = 65$ μs with probability $\alpha_1 = 0.75$ and $\alpha_2 = 0.25$ respectively, the average burst size being 50 μs again. The shape of the curves shows clear similarities with that of the ones in Figure 3, and the "local optima" induced by the predominant 45 μs burst sizes can easily be distinguished. However, the optima are not as pronounced as in the (single-valued) deterministic case, due to the presence of the 65 μs burst sizes. The "local optima" induced by the latter can be observed as "knees" in the curves. The example learns that the presence of different burst sizes alleviates the tight connection between average burst size and optimal granularity.

To conclude this section, Figure 5 shows results for varying buffer depths N. The overall shape of the curves does not change drastically with N, but the global optimum granularity can. For $N = 5$ and $N = 10$, the optimum is at $D = 45$ μs, while for $N = 20$, it is at $D = 22.5$ μs. In the latter case especially, the optimum is rather broad, so that a nearly constant BLP is observed for all values of D between 22.5 μs and 45 μs.

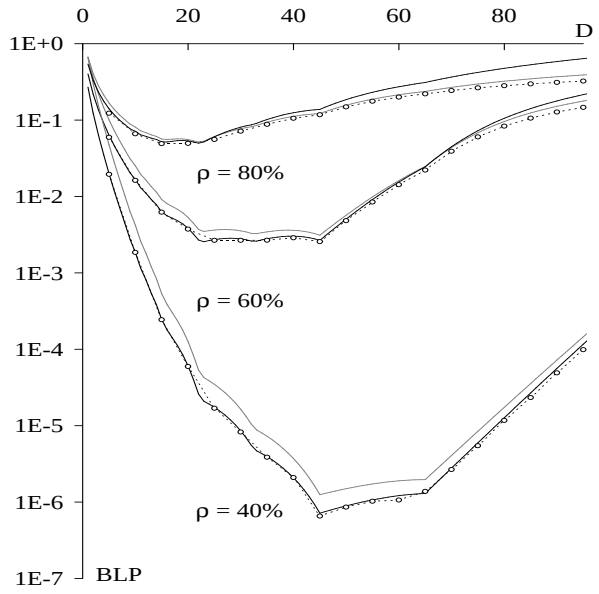

Fig. 4. BLP for a mixture of deterministic burst sizes ($N = 20$).

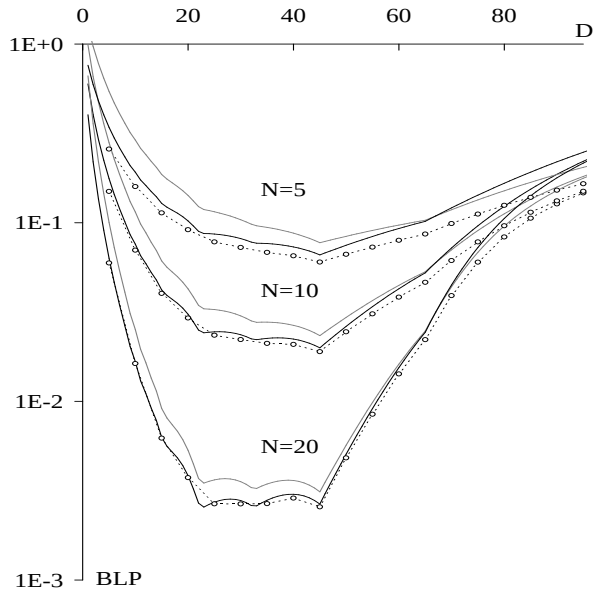

Fig. 5. BLP for a mixture of deterministic burst sizes ($\rho = 60\%$).

6 Conclusions

Expressions for various performance measures for asynchronous optical buffers were derived by taking the limit of corresponding results for synchronous ones obtained elsewhere. An analysis directly in continuous time seems feasible too, but appears to be slightly more complex than the limit procedure (at least to the authors' opinion). Heuristics were developed to determine the BLP in finite systems, based on (approximate inversion of) the LST of the scheduling

horizon in an infinite system. Three special cases of burst size distributions were used to establish the accuracy of these heuristics. For these special cases, the resulting formulas turned out to be relatively simple, i.e., not involving infinite sums, allowing for easy numerical evaluation.

The numerical examples given revealed that the BLP is rather sensitive to the choice of the granularity D, as was the case for synchronous optical buffers. The optimal granularity depends not only on the burst size distribution, but also on the offered load and the buffer depth.

In future work, the authors hope to report on results for more realistic models of optical buffers and the traffic that is offered to them. Possible extensions could consider correlated traffic, systems with multiple wavelengths at their output or systems using void-filling policies, and non-degenerate FDL structures, where the realizable delays are not necessarily a multiple of some granularity D. For some of these extensions, exact or approximate analytic results seem within reach, while for others an analytic approach might turn out to be unfeasible.

References

[1] C. Guillemot et al. Transparent optical packet switching: the European ACTS KEOPS project approach. *Journal on Lightwave Technology*, 16(12):2117–2134, 1998.

[2] D. Blumenthal. Photonic packet switching and optical label swapping. *Optical Networks Magazine*, 2(6):54–65, 2001.

[3] C. Qiao and M. Yoo. Optical burst switching–a new paradigm for an optical internet. *Journal on High-Speed Networks*, 8:69–84, 1999.

[4] J. Turner. Terabit burst switching. *Journal on High-Speed Networks*, 8:3–16, 1999.

[5] Y. Xiong, M. Vandenhoute, and H. Cankaya. Control architecture in optical burst-switched WDM networks. *IEEE Journal on Selected Areas in Communications*, 18(10):1838–1851, 2000.

[6] L. Xu, H. G. Perros, and G. Rouskas. Techniques for optical packet switching and optical burst switching. *IEEE Communications Magazine*, 39(1):136–142, 2001.

[7] S. Yao, B. Mukherjee, and S. Dixit. Advances in photonic packet switching: an overview. *IEEE Communications Magazine*, 38(2):84–94, 2000.

[8] F. Callegati. Approximate modeling of optical buffers for variable length packets. *Photonic Network Communications*, 3(4):383–390, 2001.

[9] D. Fiems, J. Walraevens, and H. Bruneel. Discrete time queueing analysis of a fibre delay line structure with granularity. *Proceedings ONDM 2004 (Ghent)*, 2004.

[10] K. Laevens and H. Bruneel. Analysis of a single-wavelength optical buffer. *Proceedings Infocom 2003 (San Fransisco)*, 2003.

[11] L. Li. *Design and Optimization of Packet Switching and Traffic Grooming in WDM Optical Networks*. PhD thesis, Lincoln University, Nebraska, 2004.

[12] W. Rogiest, K. Laevens, D. Fiems, and H. Bruneel. Analysis of an asynchronous single-wavelength FDL buffer. *Accepted for Publication in Proceedings ITC 19 (Beijing)*, 2005.

[13] K. Laevens, B. Van Houdt, C. Blondia, and H. Bruneel. Sustainable load of fibre-delay line buffers. *Electronics Letters*, 40(2):137–138, 2004.

[14] H. Bruneel and B.G. Kim. *Discrete-Time Models for Communication Systems Including ATM*. Boston: Kluwer Academic Publishers, 1993.

[15] J.C. Van Ommeren. *Asymptotic analysis of queueing systems*. PhD thesis, Vrije Universiteit te Amsterdam, 1989.

[16] K. Laevens and H. Bruneel. Analysis of fiber delay line optical buffers. *Workshop on Next Generation Networks: Architecture, Protocols, Performance (Belize)*, 2005.

[17] D. Hong, P. Poppe, J. Reynier, F. Baccelli, and G. Petit. The impact of burstification on TCP throughput in optical burst switching networks. *Proceedings ITC 18 (Berlin)*, 2003.

[18] L. Kleinrock. *Queueing Systems, Volume 1: Theory*. John Wiley & Sons, 1975.